UDC 551.506.1:551.556.8:551.465.752(267) "54"

# MONTHLY CHARTS OF SURFACE WIND STRESS CURL OVER THE INDIAN OCEAN

MICHAEL HANTEL

Meteorological Institute, University of Bonn, West Germany

## ABSTRACT

The surface wind stress curl is the forcing function in the equations of vertically integrated water transport of wind-driven ocean currents. Hence, it has become a basic quantity in theoretical oceanography. As the time dependence of all important surface quantities in the Indian Ocean is stronger than in other oceans, it is valuable to look particularly at the time variation in this region. This study presents monthly charts of the wind stress curl at the surface of the Indian Ocean from its land boundaries up to 50° S. and from 20° E. to 116° E.

Basic data were the monthly surface maps of the Koninklijk Nederlands Meteorologisch Instituut, derived from ship observations and given as 2° square means of the surface wind. The processing of the data is described in detail. In particular, small-scale fluctuations are objectively filtered out.

While earlier compilations are usually on a coarser grid (seasonal and 5° square averages), the present data have a refined time and space resolution. Therefore, they allow one to study more detailed structures. In particular, the charts show that the curl pattern in the Indian Ocean is not independent of longitude.

## 1. INTRODUCTION

Since the pioneering papers of Sverdrup (1947), Stommel (1948), and Munk (1950), several investigators have used the vertically integrated equations of motion as an approach to understanding the large-scale patterns of wind-driven ocean currents. In the 1950s, the main effort was directed toward explaining the steady motions. In more recent studies, time-dependent processes are also included. The governing equation for models of the more general latter type may be written (see, for example, Gates 1968) as

$$\frac{\partial}{\partial t}\nabla^2\psi+\frac{1}{\rho H}J(\psi,\nabla^2\psi)+\beta\frac{\partial\psi}{\partial x}-F(\psi)=\mathrm{curl}_z\,\tau. \qquad (1)$$

The $x$, $y$ coordinates are counted positive to the east and north, respectively. The $\psi=\psi(x,y,t)$ is the stream function for the horizontal mass transport components $M_x$, $M_y$ given by

$$M_x=\int_{-H}^{Z}\rho u\,dz=-\frac{\partial\psi}{\partial y},\quad M_y=\int_{-H}^{Z}\rho v\,dz=\frac{\partial\psi}{\partial x}. \qquad (2)$$

$H$ is the depth of the ocean, assumed to be constant, $Z$ the ocean's free surface ($Z<<H$), $J$ the usual Jacobian operator, $\beta$ the meridional derivative of the Coriolis parameter $f$, $\rho$ the density of water, and $\tau$ the horizontal wind stress vector at sea level. The function $F$ parameterizes friction; it varies between different models.

Under stationary and linear conditions without friction, equation (1) combined with (2) yields

$$M_y=\beta^{-1}\,\mathrm{curl}_z\,\tau. \qquad (3)$$

If the $\beta$ parameter is assumed to be constant (the $\beta$-plane approximation), this equation states that the meridional mass transport component $M_y$ is directly proportional to the curl of the wind stress. The function $M_y$, as derived from equation (3), is usually called the Sverdrup transport (Sverdrup 1947).

The general vorticity equation (1) expresses a balance between the effects of time dependence, nonlinearity, the $\beta$ effect, friction, and wind stress. The left-hand side of equation (1) depends on $\psi$, whereas the right-hand side is the independent forcing function. Thus the curl of the surface wind stress over the ocean has become a fundamental quantity in discussions of the wind-driven ocean circulation.

A few authors have published stress curl distributions as observed over the world ocean (see section 2). However, none of these gives charts on a monthly or 2° square basis. This study presents monthly mean charts of $\mathrm{curl}_z\,\tau$ over the Indian Ocean from the northern land boundaries up to 50° S. and from 20° E. to 116° E., based on the 2° square wind force data of the Koninklijk Nederlands Meteorologisch Instituut (1952), briefly called the "Dutch Atlas."

Compared to other oceans, the central and the northern parts of the Indian Ocean exhibit the most pronounced seasonal change of surface conditions (see, for example, Ramage 1968); thus it seems valuable to look at the time variation in this region in closer detail. Monthly data on a 2° square basis represent a fairly high resolution both in time and space. The charts here presented may serve as an observational background for theoretical studies in this interesting region of the world ocean.

## 2. PREVIOUS INVESTIGATIONS

The first pattern of wind stress on a global scale was given by Munk (1950). Figure 9 in his original paper shows meridional sections of zonal wind stress between 20° S. and 70° N. as (1) annual means for the Atlantic and Pacific Oceans, (2) June and November means for the Atlantic Ocean, and (3) annual means for the

TABLE 1.—*Equivalent wind speeds in meters per second*

| Beaufort | 0–0.4 | 1 | 2 | 3 | 4 | 5 | 6 | 7 |
|---|---|---|---|---|---|---|---|---|
| International 1946 | | 1.0 | 2.6 | 4.6 | 6.7 | 9.3 | 12.3 | 15.4 |
| Mintz and Dean (1952) | | 1.0 | 2.5 | 4.4 | 6.7 | 9.4 | 12.5 | |
| Verploegh (1956) | | 1.5 | 3.4 | 5.6 | 7.8 | 10.2 | 12.6 | 15.1 |
| This study (Walden 1965) | 0.3 | 1.0 | 2.8 | 4.6 | 6.8 | 9.3 | 12.0 | 14.9 |

Atlantic Ocean both east and west of 40° W. The wind stress data were calculated as 5° square means. The stress curl, given for zonal winds by $-\partial\tau_x/\partial y$ can be calculated from this figure.

Mintz and Dean (1952) constructed fields of the surface wind vorticity for the world ocean. Their figures 14 and 15 show the vorticity of the January and July surface wind over the oceans, in units of $10^{-6}$ $sec^{-1}$, between 50° S. and 60° N. These patterns were computed from 5° square means of the surface wind in Beaufort; for the conversion from wind force to wind speed, see table 1. Using $\mathbf{V}=(u, v)$ as the actual horizontal vector wind and an overbar as the operator of time-averaging over a month, they calculated the wind vorticity using the formula

$$\overline{\text{curl}_z\mathbf{V}}=\text{curl}_z\overline{\mathbf{V}}. \quad (4)$$

The main features of the global surface vorticity are discussed best in terms of a meridional section of the zonally averaged fields (fig. 16 of Mintz and Dean 1952). The figure shows, briefly, anticyclonic vorticity in middle and subtropical latitudes and cyclonic vorticity in the Tropics. The general cyclonic vorticity in tropical latitudes is interrupted by a narrow band of anticyclonic vorticity just north of the Equator in July and just south of the Equator in January. They attributed this effect to the recurving of the southeasterly trades at the Equator in July and to the recurving of the northeasterly trades in January.

The Indian Ocean, however, is an exception to these general features; only the January field is in agreement. The Indian Ocean summer vorticity, on the other hand, shows considerable deviations from the normal pattern. Areas of strong negative (anticyclonic) vorticity cover almost the entire northern Indian Ocean—apart from comparatively small positive areas close to the coast of Arabia and the east coast of India—and display an impressive anomaly of the vorticity distribution. These observations demonstrate that the Indian Ocean north of 10° S. has stronger seasonal vorticity changes than any other area of the world ocean.

For avoiding confusion, it should be noted that the fields of $\text{curl}_z\mathbf{V}$ (wind vorticity) and $\text{curl}_z\tau$ (wind stress curl) exhibit similar patterns. Figure 1A shows the wind vorticity, and figure 1B the stress curl, computed from the same data, for the month of July. Because of the similarity of the two distributions, it does not seem inappropriate to

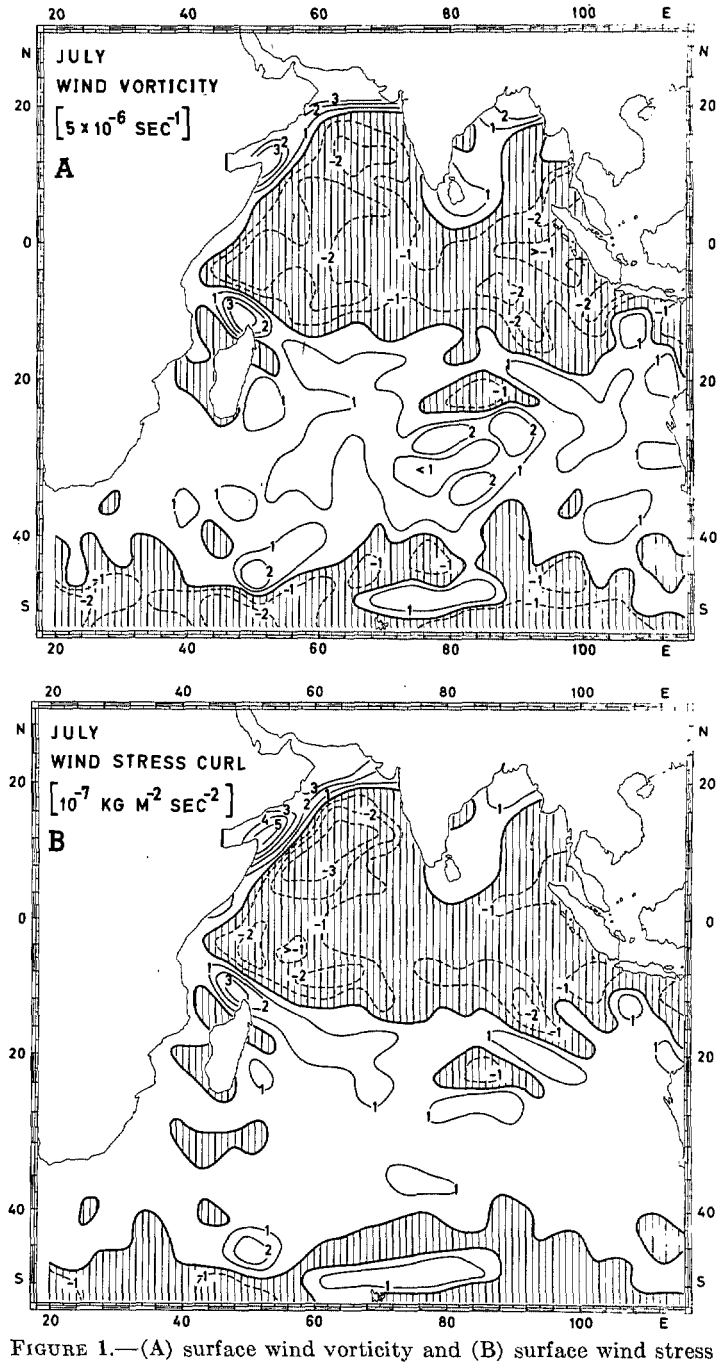


FIGURE 1.—(A) surface wind vorticity and (B) surface wind stress curl, both over the Indian Ocean for July. The negative areas are shaded.

compare compilations of wind vorticity and stress curl done by different authors.

Stommel (1965) published a summary paper of several sea-surface quantities, including maps of the annual mean wind stress and the wind stress curl. They cover the world ocean between approximately 50° S. and 50° N. The stress and the stress curl were drawn from the tables of Hidaka (1958); these tables contain seasonal and annual means of the surface wind stress, calculated for 5° square areas. Stommel obtained approximately the same annual stress curl distributions as Mintz and Dean did in their winter

and summer vorticity fields. In Stommel's annual map, the strongest deviation from this pattern also occurs in the Indian Ocean north of the Equator. Except for a positive curl area between Ceylon and Sumatra, this whole region has negative curl. This is an effect of the strong summer circulation which overbalances the positive winter curl.

In a recent paper by Holopainen (1967), the annual mean wind stress curl was calculated for the Northern Hemisphere north of 10° N. His investigation is noteworthy for a different approach to the surface curl. While other authors—including the present one—derive the curl from surface observations, requiring assumptions about the drag coefficient, Holopainen determines the vorticity budget of the whole atmosphere. Vertical integration of the atmospheric vorticity equation between the upper ($p_0$=100 mb) and the lower ($p_s$=1000 mb) boundaries of the atmosphere gives the mean surface wind stress curl over the ocean as

$$\mathrm{curl}_z\,\tau_s = -\frac{1}{g}\int_{p_0}^{p_s}\overline{\mathbf{V}\nabla\eta}\,dp. \tag{5}$$

In this equation, $\eta=\zeta+f$ is the absolute wind vorticity, $\zeta$ the relative vorticity, $f$ the Coriolis parameter, and $\mathbf{V}=(u,v)$ the horizontal wind vector. Numerical evaluation of the integral in equation (5) was based on the charts of Crutcher (1959). The $\mathrm{curl}_z\,\tau_s$ values were plotted in the unit $10^{-7}$ kg m$^{-2}$ sec$^{-2}$ as in the present study. The pattern over the oceans compares satisfactorily with the map of Stommel (1965), especially in the North Atlantic and in the Indian Ocean north of 12° N. On the basis of a barotropic frictional layer theory, Holopainen states a linear relationship between the annual mean wind stress curl and the wind vorticity at the surface. This will allow a close comparison of the annual fields of $\mathrm{curl}_z\,\tau$ and $\mathrm{curl}_z\,\mathbf{V}$ in middle latitudes. Near the Equator, this theory does not apply because the proportionality factor depends on $\sqrt{f}$. From the field of the wind stress curl and with the aid of equations (2) and (3), Holopainen derived the stream function for the Sverdrup transport in both the North Atlantic and North Pacific Oceans. For the Indian Ocean, no such calculation was made.

## 3. THE DUTCH ATLAS

Publication No. 135 of the Koninklijk Nederlands Meteorologisch Instituut (1952), in this study referred to as the Dutch Atlas, provides 12 monthly sheets of sea-surface observation of mean wind arrows (direction in 5° intervals and force in Beaufort). The wind values were based on ship observations and averaged over 2° square fields. No data were given for 2° squares with fewer than five separate observations. For most of these fields, more than 24 separate observations were available.

The Dutch Atlas also provides 12 monthly sheets with more oceanographically oriented data, in particular sea-surface currents (direction and speed). The atlas contains additional fields of surface air pressure, temperature (air and water), and storm tracks. Verploegh (1960) discusses in some detail the annual variation of the pressure, the air and sea temperatures, and the wind system. His five meridional sections of the annual variation of the surface wind show in particular the constancy of the wind, as defined by the ratio of the vector mean to the scalar mean.

## 4. CONVERSION OF WIND FORCE TO WINDSPEED AND STRESS

The relationship between wind force in Beaufort and windspeed in meters per second has been under discussion for decades. For references, see Verploegh (1956, 1967) and Walden (1965). Both investigators summarize the possible errors in wind measurement aboard ship: measured quantities may be in error due to the influences of anemometer height, air stability, wind gusts, and relative velocity differences induced by the ship's pitch and roll. Sources of error in an observer's estimates are the wind direction relative to the ship's travel, his own height relative to the sea surface, the duration of a single observation, the kind of wind effects observed (foam, waves, sound of the rigging) and, of course, an inevitable subjectivity even in experienced observers.

From an extensive comparison of these errors, Verploegh (1967) is led to the important conclusion that "the accidental errors of wind measurement have the same order of magnitude as those of wind estimates." This order of magnitude is 0.58 $I$, where $I$ is the Beaufort interval. Furthermore, by comparing different observing techniques, Verploegh concludes with the general rule that "observers who are accustomed to their surroundings, i.e., experienced in observing wind effects on environmental objects, will be able to distinguish mean wind speeds to the same degree of precision whatever wind effects are observed." These results should demonstrate the usefulness of wind force data obtained by simple observation. The conversion scale of this study (table 1) has been adopted from Walden (1965); it closely resembles the international scale of 1946 (Walden 1965).

The conversion from windspeed to wind stress is also an unsolved problem. A simple formula valid for all ocean regions does not exist. In the past, a jump in the drag coefficient at Beaufort 4 was often assumed (Munk 1947). For his above-mentioned wind stress tables, Hidaka (1958) uses a formula with $C_D=0.8\times10^{-3}$ for winds below 6.6 m sec$^{-1}$ and $C_D=2.6\times10^{-3}$ for winds above this speed. Some stress values according to this formula are listed in table 2. Hellerman (1967), in his updated estimate of the wind stress on the world ocean, adopted a $C_D$ table with a 40 percent jump at Beaufort 4. Hellerman also takes into account latitudinal variations of the air density. An estimate of his stress values, based on the equivalent wind velocity values of the last line of table 1, is summarized in table 2.

TABLE 2.—*Equivalent wind stress values in $10^{-1}$ kg $m^{-1}$ $sec^{-2}$*

| Beaufort | 0-0.4 | 1 | 2 | 3 | 4 | 5 | 6 | 7 |
|---|---|---|---|---|---|---|---|---|
| Hidaka (1958) | 0.001 | 0.01 | 0.08 | 0.22 | 1.56 | 2.92 | 4.87 | 7.50 |
| Hellerman (1967) | 0.001 | 0.01 | 0.08 | 0.24 | 0.74 | 2.16 | 4.30 | 6.75 |
| This study | 0.001 | 0.02 | 0.13 | 0.34 | 0.74 | 1.38 | 2.30 | 3.55 |

Other recent investigations tend to use constant drag coefficients. The $C_D$ plot by Weiler and Burling (1967) shows no systematic decrease or increase of this quantity in the range 1.5 to 10.5 m $sec^{-1}$, though large scattering—at least 50 percent—is evident. Hasse (1968), both from his own measurements and from a comparison of the results of several earlier authors, comes to the conclusion that in the windspeed range 2 to 12 m $sec^{-1}$ the relationship

$$|\tau| = C_D \rho |\mathbf{V}|^2 \tag{6}$$

will nearly hold with constant $C_D$. The values of $C_D$ summarized by Hasse (see his fig. 3) are valid for 10-m heights above sea level. They are in the range 1.0 to $1.3 \times 10^{-3}$, with individual errors of 17 to 28 percent. The conversion table between Beaufort force and wind stress, using equation (6) with $C_D = 1.2 \times 10^{-3}$ and $C_D \rho = 1.6 \times 10^{-3}$ kg $m^{-3}$, was adopted in the present study and is listed in table 2 (note 1 kg $m^{-1}$ $sec^{-2}$ = 10 dynes $cm^{-2}$).

In the numerical calculations of this study, the Beaufort values were converted into the absolute magnitude $|\tau|$ of the respective wind stress values. The wind stress components were calculated with the aid of the simple relations

$$\tau_x = |\tau| \sin \alpha, \tau_y = |\tau| \cos \alpha \tag{7}$$

where $\alpha$ is the angle between north and the direction of the wind vector. It may be noted that no shift between the direction of the wind and the wind stress has been taken into consideration.

Figure 2 shows four meridional sections of the zonal wind stress component in the western and the eastern parts of the Indian Ocean for both winter and summer. The curves represent the results of this study, while the arrows are redrawn from the Hellerman tables. The data have been zonally averaged over an array of 10° longitude; the curves and the arrows are representative for the longitude intervals 60°–70° E. and 80°–90° E., respectively. Additionally, for obtaining the "winter" curves, the stress data computed from the Dutch Atlas for December, January, and February have been averaged; the "summer" curves are averages obtained from the June, July, and August data. The magnitude of the arrows are indicated by the scale on top of the figure; the scale on the bottom is to be used for the curves.

Though the patterns of figure 2 seem to fit roughly, the differences are noteworthy. They arise mainly from the different conversion tables (table 2). Part of the differences stem from the fact the Hellerman's stress data are based on wind roses with speed frequency information; whereas

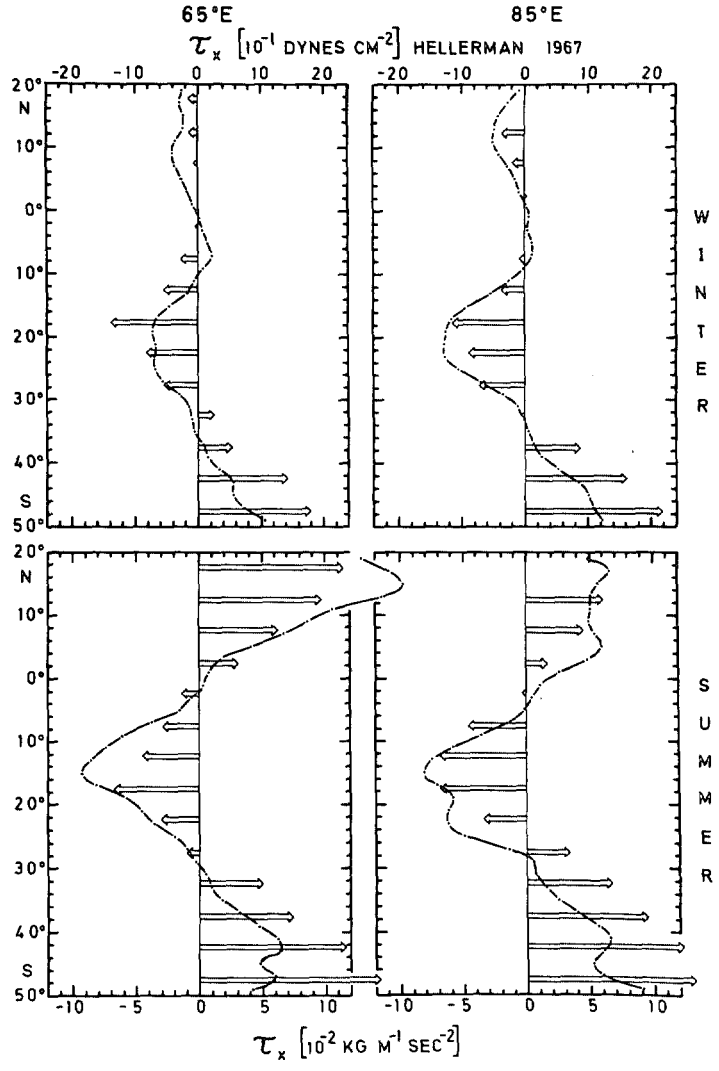


FIGURE 2.—Meridional distribution of the zonal wind stress component in the western (65° E.) and eastern (85° E.) parts of the Indian Ocean; upper diagrams for January, lower diagrams for July. Scale on top of the diagrams is valid for the arrows (Hellerman 1967); scale on the bottom is valid for the curves (present study).

in the present study, the stress is calculated from the mean wind. On the other hand, the time and space grid of Hellerman (5° square seasonal averages) is coarser than the grid of this study (2° square monthly averages). In any case, the differences of the two methods should be small in regions with high wind constancy. The maps of Verploegh (1960) show that in July the constancy over the latitude range 20° N.–20° S. is greater than 60 percent; over most of the range, it is even greater than 74 percent. Hence, the fit in figure 2 is relatively good in the entire area. Conversely, the poor agreement south of latitude 30° S. is related to a minimum of wind constancy between 30°–40° S. (constancy <25 percent).

## 5. SUPPLEMENTING OF DATA, OBJECTIVE FILTERING

As mentioned previously, some 2° square fields of the monthly wind maps contain fewer than five separate ob-

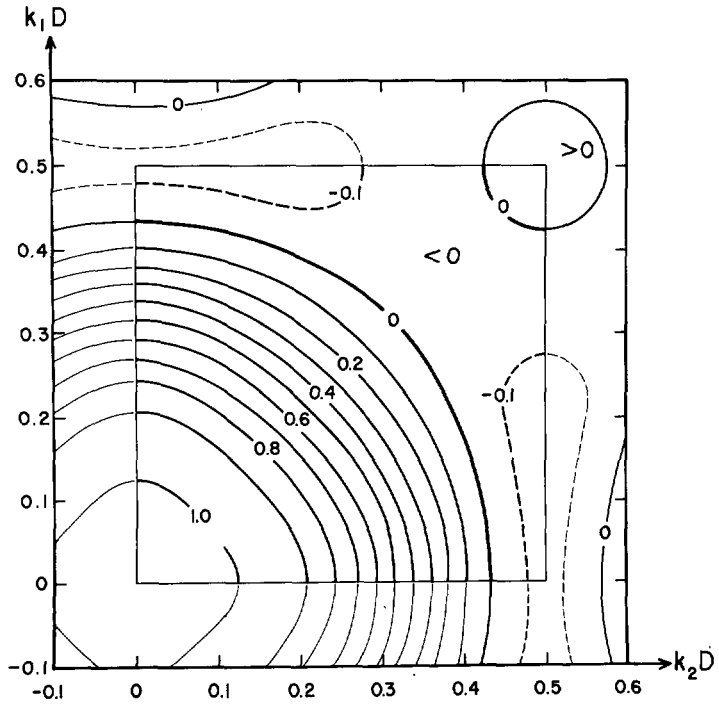


FIGURE 3.—Wave number response function, according to Bleck (1965). Nyquist wave number $kD=0.5$. The function is completely determined by the values inside the interior square.

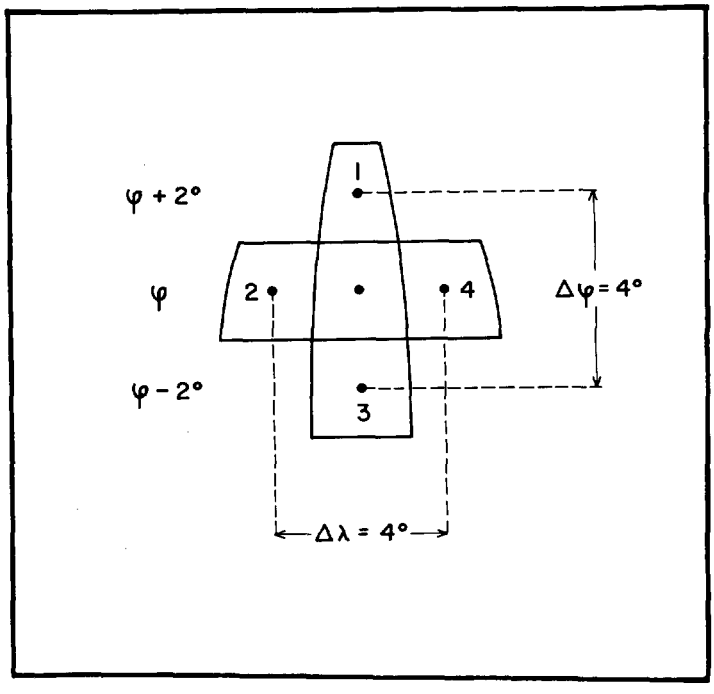


FIGURE 4.—Discretization grid for the finite-difference curl operator.

servations. In these cases, no wind arrows were drawn in the Dutch Atlas. In the curl charts (fig. 5), such squares are denoted by dots.

The missing values of $\tau_x$ and $\tau_y$ were obtained by linear interpolation in the zonal direction. There exists, in fact, a linear trend of the wind stress components in zonal direction over distances of a few grid points. To use data from other sources did not seem possible since the available data are valid for larger averaging scales.

The completed patterns of $\tau_x$, $\tau_y$ were smoothed by an objective filtering method. The following discrete weight function $w(\alpha_1 D, \alpha_2 D)$ derived by Bleck (1965) was applied.

$$\begin{array}{cccccc} w(-2,\ 2) & w(-1,\ 2) & w(\ 0,\ 2) & w(\ 1,\ 2) & w(\ 2,\ 2) \\ w(-2,\ 1) & w(-1,\ 1) & w(\ 0,\ 1) & w(\ 1,\ 1) & w(\ 2,\ 1) \\ w(-2,\ 0) & w(-1,\ 0) & w(\ 0,\ 0) & w(\ 1,\ 0) & w(\ 2,\ 0) \\ w(-2,-1) & w(-1,-1) & w(\ 0,-1) & w(\ 1,-1) & w(\ 2,-1) \\ w(-2,-2) & w(-1,-2) & w(\ 0,-2) & w(\ 1,-2) & w(\ 2,-2) \end{array}$$

The weight function is symmetrical and equal in both the zonal and meridional directions; hence only the values in the dashed box need be listed here. These are given by

$$\left.\begin{array}{llll} w(0,0) = & 0.279372 & w(1,0) = & 0.171943 \\ w(2,0) = & -0.006918 & w(1,1) = & 0.077458 \\ w(2,1) = & -0.024693 & w(2,2) = & -0.012940 \end{array}\right\} \quad (8)$$

where $w$ is normalized to conserve the mean value of the smoothed pattern. The pertinent wave number response function for this linear operator is defined by

$$H(k_1, k_2) = \sum_{\alpha_1,\ \alpha_2=-N}^{N} w(\alpha_1 D, \alpha_2 D) \times e^{2\pi i(\alpha_1 k_1 + \alpha_2 k_2) D}. \quad (9)$$

$D$ (equals 2° latitude or longitude) is the grid distance, $k_1$ and $k_2$ are the wave numbers in both directions, given in terms of $1/D$ (thus the $kD$ are dimensionless), and $\alpha_1$ and $\alpha_2$ are the grid-point indices; $N$ is set equal to 2. The wave number response is a space analog to the familiar frequency response. Figure 3 shows a plot of the wave number response, which is, of course, even in both directions with respect to 0. Due to the symmetry of the weight function, the response is a real function. Phase shift occurs only in areas where $H$ has negative values; in these areas, the phase shift is 180°.

## 6. CALCULATION OF WIND STRESS CURL

The vertical component of the curl of a vector $\tau = (\tau_x, \tau_y)$ is given by

$$\mathrm{curl}_z \tau = \frac{1}{R \cos\phi} \left\{ \frac{\partial \tau_y}{\partial \lambda} - \frac{\partial}{\partial \phi} (\tau_x \cos\phi) \right\} \quad (10)$$

where $R$ denotes the radius of the earth and $\phi$ and $\lambda$ denote geographical latitude and longitude, respectively. The following discretization formula has been used (note $\Delta\lambda = \Delta\phi$) to approximate the curl value for the middle 2° square of figure 4:

$$\mathrm{curl}_z \tau \approx \frac{1}{R \cos\phi \, \Delta\phi} \{ \tau_{y4} - \tau_{y2} - \tau_{x1} \cos(\phi + 2°) + \tau_{x3} \cos(\phi - 2°) \}. \quad (11)$$

For typical wind stress values of $10^{-1}$ kg m$^{-1}$ sec$^{-2}$ and

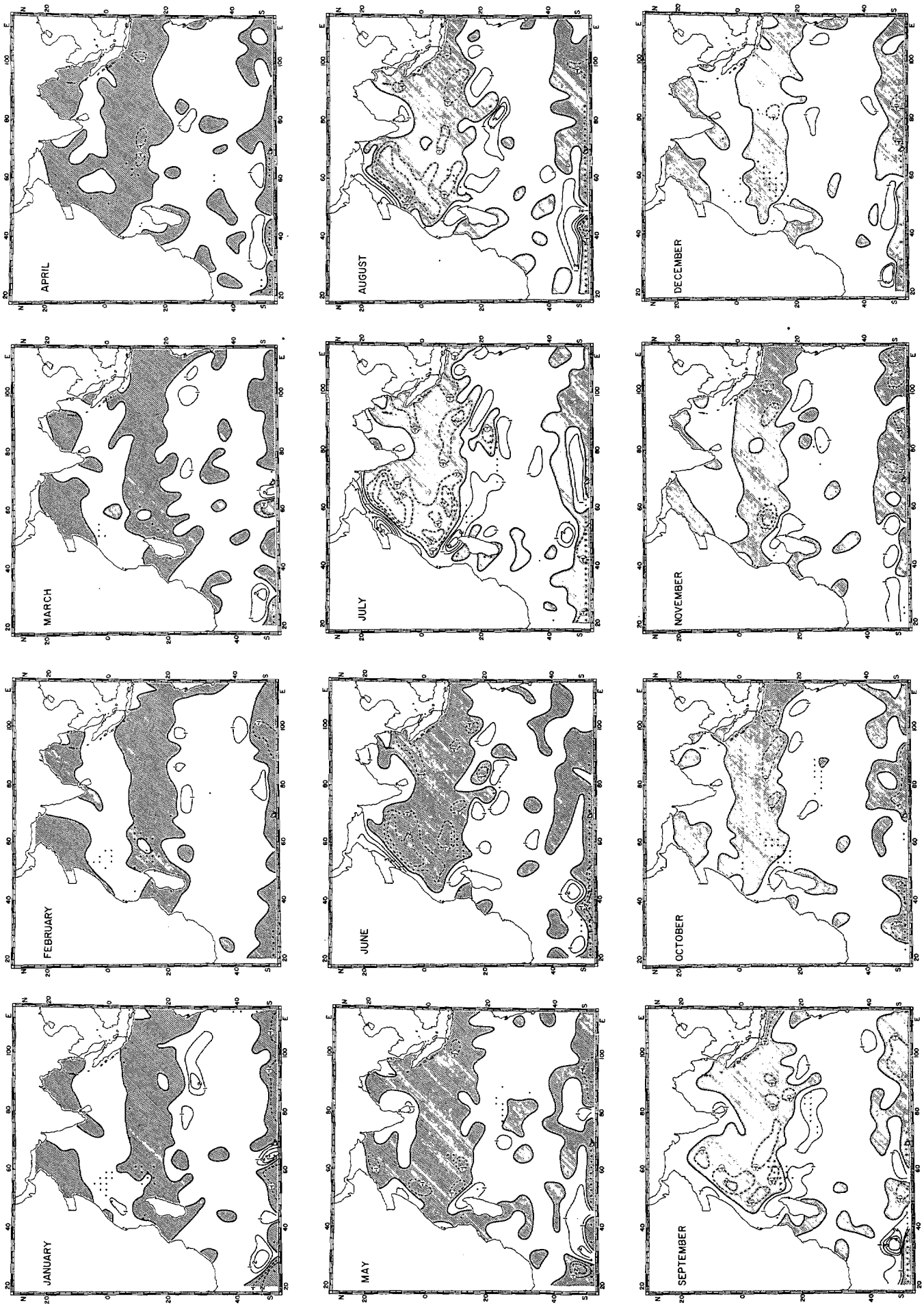


FIGURE 5.—Surface wind stress curl over the Indian Ocean. Units, $10^{-7}$ kg m$^{-2}$ sec$^{-2}$ = $10^{-8}$ dynes cm$^{-3}$. Negative areas are shaded. Dots indicate 2° squares without available wind data.

with $R \cos\phi \Delta\phi \simeq 4 \times 10^5$ m, typical values for the wind stress curl are of the order $2.5 \times 10^{-7}$ kg m$^{-2}$ sec$^{-2}$ $= 2.5 \times 10^{-8}$ dynes cm$^{-3}$.

## 7. MONTHLY CHARTS OF WIND STRESS CURL OVER THE INDIAN OCEAN

Figure 5 shows the mean monthly distribution of the curl of the surface wind stress. The isolines are in units of $10^{-7}$ kg m$^{-2}$ sec$^{-2}$.

During winter, curl values of the order of one predominate over the entire Indian Ocean. Positive values are generally observed in the region north of 0° to 10° S. However, there are relatively large negative areas in the northwestern Arabian Sea and in the northwestern Bay of Bengal. South of latitude 5° S., a 15° to 20° wide zonal band of negative curl runs from East Africa to Indonesia-Australia. South of this band, positive values prevail to 45° S., where again negative values begin to occur. This pattern predominates more or less from November until March.

During summer (May through September), the curl field north of 0° to 10° S. is reversed in sign and is remarkably strengthened in intensity—by a factor of 2 at least. Over the entire region north of 10° S., negative curl appears, with values as low as −3 in midsummer in the central Arabian Sea. A narrower coastal strip 100 to 600 km wide, running from Madagascar along the coasts of East Africa, Arabia, and India, has mostly strong positive values—up to +5.

It does not seem suitable to dwell on the small-scale details of the curl fields since the smoothing procedure tends to blur them. Likewise, one should exercise caution in accounting for the patterns close to the boundaries.

Two large-scale features seem to be interesting. First is the belt of strong positive curl running northwest-southeast from Dar es Salaam along the northern tip of Madagascar to 20° N., 60° E. This belt is observed from April until December, its intensity varying and reaching a maximum in July. Second is a zone of negative (i.e., cyclonic) wind stress curl arising south of 45° S. This is in agreement with Mintz and Dean (1952) insofar as these authors stated from the observation of mean westerly current in 50° latitude and from the application of Stokes' theorem that the vector means of the vorticity over the entire polar caps should be cyclonic in sign. For the northern polar cap, the mean annual curl map of Holopainen (1967) also shows cyclonic (that is, positive) wind stress curl.

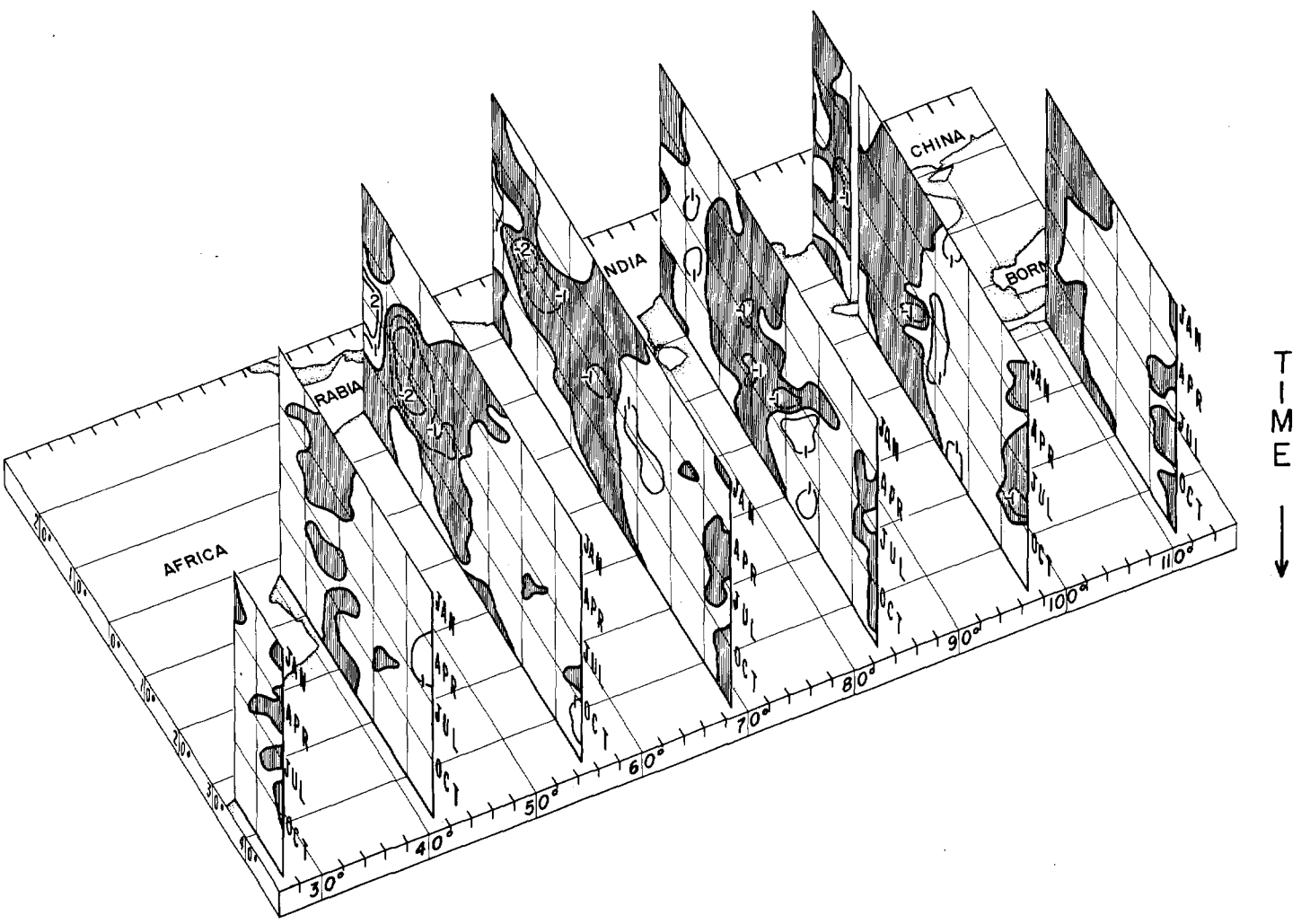


FIGURE 6.—Surface wind stress curl over the Indian Ocean on several latitude-time sections, redrawn from figure 5.

## 8. CONCLUSIONS

This study is intended to give a picture of the annual shift of the surface wind stress curl over the Indian Ocean down to 50° S., based on surface ship observations as presented in the 2° square monthly maps of the Dutch Atlas. Although it is not believed that the plots of figure 5 are final, they may provide more insight into the complex time-dependent structure of the curl pattern over this part of the ocean.

For inferring the time changes, figure 6 displays seven latitude-time sections. The sections are equidistant, and the time scale is positive downward. The stress curl unit is as in figure 5. The figure exhibits 14 percent of the information contained in the whole set of the 12 monthly charts. The strong time-dependent areas are indicated by nearly horizontally running isolines, most pronounced over the Arabian Sea (sections 55° E. and 69° E.).

The presented curl data may be useful in establishing wind-driven ocean models based on the time-dependent vorticity equation (1). Recently, Düing (1968) has discussed such a model for the Indian Ocean. He used a stress curl pattern of the following type

$$\mathrm{curl}_z \tau = \left(a \sin \frac{y}{y_0} + b\right) e^{i\omega t} \qquad (12)$$

where $y$ is a latitudinal coordinate and $a$, $b$, and $y_0$ are constants. Thus the curl varies harmonically both with latitude and with time; $\omega$ corresponds to a period of 1 yr. Zonal gradients of the wind stress curl are not included in equation (12). Obviously, functions of this type fit the observed curl pattern in the central Indian Ocean to a limited degree only. As can be seen by inspection of figures 5 or 6, the zonal gradient of the wind stress curl is not negligible; it can even be larger than the pertinent meridional gradient.

Due to the time lag between the driving forces and the response of the ocean, the calculation of Sverdrup transport charts from the presented curl fields does not seem meaningful. The time lag for barotropic processes is of the order of 1 mo (Hantel 1969).

Another well-known application of the surface stress curl field is concerned with upwelling. At the bottom of the divergent surface Ekman layer of the ocean, an estimation of the vertical velocity is

$$w = \frac{1}{\rho f} \mathrm{curl}_z \tau. \qquad (13)$$

Positive vertical velocities should be connected with negative anomalies of sea-surface temperature. Indeed, the strong positive curl values in the northern summer near the Somali coast, considerably north of the Equator, are accompanied by the well-known negative temperature anomalies off this coast. The negative curl values in the Southern Hemisphere between Madagascar and the African coast in August and September may also be accompanied by negative temperature anomalies during late summer and fall (Miller and Jefferies 1967).

### ACKNOWLEDGMENTS

The author is indebted to Prof. H. Flohn, Director of the Meteorological Institute of the University of Bonn, West Germany, for continuing stimulation during the preparation of this work. The numerical calculations were carried out on the IBM 7090 computer of the Institute of Applied Mathematics of the University of Bonn. The manuscript was prepared mainly during the author's stay at the Institute of Atmospheric Sciences of the University of Miami, Fla., on a fellowship granted by the Heinrich-Hertz-Foundation of the State Nordrhein-Westfalen, West Germany. The author is indebted to Drs. E. B. Kraus, C. Rooth, J. Geisler, and D. Latham for challenging discussions, and to Dr. M. A. Estoque and Mrs. B. Wallbrecher for reading the manuscript. The drawings were done by Miss B. Eggemann, Miss H. Lichtenfeld, and Mr. W. Schmitz-Luck in Bonn, and by Mr. G. Posada in Miami. This work was supported in part by National Science Foundation Grant GA 1455.

### REFERENCES

Bleck, Rainer, *Lineare Approximationsmethoden zur Bestimmung ein-und zweidimensionaler numerischer Filter der dynamischen Meteorologie* (Linear Approximation Methods for the Determination of One- and Two-Dimensional Numerical Filters in Dynamic Meteorology), Institut für Theoretische Meteorologie, Freie Universität, Berlin, **1965**, 86 pp.

Crutcher, H. L., "Upper Wind Statistics Charts of the Northern Hemisphere," *NAVAER* 50–1C–535, Vol. 1, U.S. Office of Naval Operations, Washington, D.C., Aug. **1959**, 33 pp.

Düing, Walter, "The Monsoon Regime of the Currents in the Indian Ocean," Department of Oceanography, University of Hawaii, Honolulu, **1968**, 81 pp. (unpublished manuscript).

Gates, W. Lawrence, "A Numerical Study of Transient Rossby Waves in a Wind-Driven Homogeneous Ocean," *Journal of the Atmospheric Sciences*, Vol. 25, No. 1, Jan. **1968**, pp. 3–22.

Hantel, Michael, "A Numerical Investigation of the Linear Primitive Equations Applied to the Wind-Driven Circulation of the Northwestern Indian Ocean Between 16°N–16°S," *Annalen der Meteorologie, Neue Folge*, No. 4, Deutscher Wetterdienst, Offenbach, Germany, Apr. 1–6, **1969**, pp. 73–76.

Hasse, G., "Zur Bestimmung der vertikalen Transporte von Impuls und fühlbarer Wärme in der wassernahen Luftschicht auf See" (On the Determination of the Vertical Transport of Momentum and Sensible Heat in the Air Layer Next to the Sea), *Hamburger Geophysikalische Einzelschriften* No. 11, *Geophysikalisches Institut der Universität* Hamburg, Germany, **1968**, 70 pp.

Hellerman, S., "An Updated Estimate of the Wind Stress on the World Ocean," *Monthly Weather Review*, Vol. 95, No. 9, Sept. **1967**, pp. 607–626 (See also "Correction Notice," Vol. 96, No. 1, Jan. 1968, pp. 63–74).

Hidaka, Koji, "Computation of the Wind Stresses Over the Oceans," *Records of Oceanographic Works in Japan*, Vol. 14, No. 2, Tokyo, **1958**, pp. 77–123.

Holopainen, G. O., "A Determination of the Wind-Driven Ocean Circulation From the Vorticity Budget of the Atmosphere," *Pure and Applied Geophysics*, Vol. 67, Basel, Switzerland, **1967**, pp. 156–165.

Koninklijk Nederlands Meteorologisch Instituut, "Indian Ocean, Oceanographic and Meteorological Data," Publication No. 135, 2d edition, 2 vols., **1952** (24 sheets).

Miller, Forrest R., and Jefferies, C., "Mean Monthly Sea-Surface Temperatures of the Indian Ocean During the International Indian Ocean Expedition," *Report* No. 2, NSF Grant GA–386, Hawaii Institute of Geophysics, Honolulu, July **1967**, 6 pp. plus figures.

Mintz, Yale, and Dean, Gordon, "The Observed Mean Field of Motion of the Atmosphere," *Geophysical Research Papers* No. 17, U.S. Air Force Cambridge Research Center, Cambridge, Mass., Aug. **1952**, 65 pp.

Munk, Walter H., "A Critical Wind Speed for Air-Sea Boundary Processes," *Journal of Marine Research*, Vol. 6, No. 3, **1947**, pp. 203–218.

Munk, Walter H., "On the Wind-Driven Ocean Circulation," *Journal of Meteorology*, Vol. 7, No. 2, Apr. **1950**, pp. 79–93.

Ramage, C. S., "Problems of a Monsoon Ocean," *Weather*, Vol. 23, No. 1, Jan. **1968**, pp. 28–37.

Stommel, Henry, "The Westward Intensification of Wind-Driven Ocean Currents," *Transactions of the American Geophysical Union*, Vol. 29, No. 2, Apr. **1948**, pp. 202–206.

Stommel, Henry, "Summary Charts of the Mean Dynamic Topography and Current Field at the Surface of the Ocean, and Related Functions of the Mean Wind-Stress," *Studies on Oceanography*, University of Washington Press, Seattle, **1965**, pp. 53–58.

Sverdrup, H. U., "Wind-Driven Currents in a Baroclinic Ocean; With Application to the Equatorial Currents of the Eastern Pacific," *Proceedings of the National Academy of Sciences*, Vol. 33, No. 11, Nov. **1947**, pp. 318–326.

Verploegh, G., "The Equivalent Velocities for the Beaufort Estimates of the Wind Force at Sea," *Mededelingen en Verhandelingen* No. 66, Meteorologisch Instituut, Koninklijk, Netherlands, **1956**, 38 pp.

Verploegh, G., "On the Annual Variation of Climatic Elements of the Indian Ocean," *Mededelingen en Verhandelingen* No. 77, Meteorologisch Institituut, Koninklijk, Netherlands, **1960**, 64 pp. and 28 charts.

Verploegh, G., "Observation and Analysis of the Surface Wind Over the Ocean," *Mededelingen en Verhandelingen* No. 89, Meteorologisch Instituut, Koninklijk, Netherlands, **1967**, 67 pp.

Walden, Hans, "Die Windgeschwindigkeits-Äquivalente der Beaufortgrade nach Beobachtungen deutscher Bordwetterwarten" (The Equivalents of the Wind Velocity for the Beaufort Numbers as Derived From Observations of German Ship-Borne Meteorological Stations), *Einzelveröffentlichungen* No. 47, Seewetteramt, Hamburg, **1965**, 70 pp.

Weiler, H. S., and Burling, K. W., "Direct Measurements of Stress and Spectra of Turbulence in the Boundary Layer Over the Sea," *Journal of the Atmospheric Sciences*, Vol. 24, No. 6, Nov. **1967**, pp. 653–664.

[*Received September 9, 1969; revised March 30, 1970*]